Could a change in magnetic field geometry cause the break in the wind-activity relation?

A. A. Vidotto,[1][*] J.-F. Donati,[2,3] M. Jardine,[4] V. See,[4] P. Petit,[2,3] I. Boisse,[5] S. Boro Saikia,[6] E. Hébrard,[2,3] S. V. Jeffers,[6] S. C. Marsden[7] and J. Morin[8]

[1]*Observatoire de l'Université de Genève, Chemin des Maillettes 51, Versoix CH-1290, Switzerland*
[2]*Université de Toulouse, UPS-OMP, IRAP, 14 avenue E. Belin, Toulouse F-31400, France*
[3]*CNRS, IRAP / UMR 5277, Toulouse, 14 avenue E. Belin F-31400, France*
[4]*SUPA, School of Physics and Astronomy, University of St Andrews, North Haugh, St Andrews KY16 9SS, UK*
[5]*LAM-UMR 7326, Aix Marseille Université, Laboratoire d'Astrophysique de Marseille, F-13388 Marseille, France*
[6]*Institut für Astrophysik, Georg-August-Universität, Friedrich-Hund-Platz 1, D-37077 Goettingen, Germany*
[7]*Computational Engineering and Science Research Centre, University of Southern Queensland, Toowoomba 4350, Australia*
[8]*LUPM-UMR5299, Université Montpellier II, Place E. Bataillon, Montpellier F-34095, France*

ABSTRACT

Wood et al. suggested that mass-loss rate is a function of X-ray flux ($\dot{M} \propto F_x^{1.34}$) for dwarf stars with $F_x \lesssim F_{x,6} \equiv 10^6$ erg cm^{-2} s^{-1}. However, more active stars do not obey this relation. These authors suggested that the break at $F_{x,6}$ could be caused by significant changes in magnetic field topology that would inhibit stellar wind generation. Here, we investigate this hypothesis by analysing the stars in Wood et al. sample that had their surface magnetic fields reconstructed through Zeeman–Doppler Imaging (ZDI). Although the solar-like outliers in the $\dot{M} - F_x$ relation have higher fractional toroidal magnetic energy, we do not find evidence of a sharp transition in magnetic topology at $F_{x,6}$. To confirm this, further wind measurements and ZDI observations at both sides of the break are required. As active stars can jump between states with highly toroidal to highly poloidal fields, we expect significant scatter in magnetic field topology to exist for stars with $F_x \gtrsim F_{x,6}$. This strengthens the importance of multi-epoch ZDI observations. Finally, we show that there is a correlation between F_x and magnetic energy, which implies that $\dot{M}$ – magnetic energy relation has the same qualitative behaviour as the original $\dot{M} - F_x$ relation. No break is seen in any of the F_x – magnetic energy relations.

Key words: magnetic fields – stars: activity – stars: coronae – stars: low-mass – stars: winds, outflows.

1 INTRODUCTION

Like the Sun, low-mass stars experience mass-loss through winds during their entire lives. Although the solar wind can be probed *in situ*, the existence of winds on low-mass stars is known indirectly, e.g. from the observed rotational evolution of stars (see Bouvier et al. 2014, and references therein). Measuring the wind rates $\dot{M}$ of cool, low-mass stars is not usually an easy task though. Although in their youth, when the stars are still surrounded by accretion discs, their winds have been detected (Gómez de Castro & Verdugo 2007; Kwan, Edwards & Fischer 2007), this is no longer the case after their accretion discs dissipate. The belief is that, from the dissipation of the disc onwards, winds of low-mass stars are no longer as dense, making it more difficult to detect them directly.

There have been several attempts to detect radio free–free thermal emission from the winds of low-mass stars. The lack of detection means that only upper limits in $\dot{M}$ can be derived (e.g. van den Oord & Doyle 1997; Gaidos, Güdel & Blake 2000; Villadsen et al. 2014). Detecting X-ray emission generated when ionized wind particles exchange charges with neutral atoms of the interstellar medium has also been considered, but again only upper limits on $\dot{M}$ could be derived (Wargelin & Drake 2002). Other methods, involving the detection of coronal radio flares (Lim & White 1996) or the accretion of wind material from a cool, main-sequence component to a white dwarf component (Debes 2006; Parsons et al. 2012), have also been suggested. However, the indirect method of Wood et al. (2001) has been the most successful one, enabling estimates of $\dot{M}$ for about a dozen dwarf stars.

This method assumes that the observed excess absorption in the blue wing of the H I Lyman α line is caused by the hydrogen wall that forms when the stellar wind interacts with the interstellar

*E-mail: Aline.Vidotto@unige.ch

medium. Unfortunately, this method requires high-resolution UV spectroscopy, low-H I column density along the line of sight and a suitable viewing angle of the system (Wood et al. 2005a), making it difficult to estimate $\dot{M}$ for a large number of stars. Wood et al. (2002, 2005b) showed that, for dwarf stars, there seems to be a relationship between the mass-loss rate per unit surface area $A_\star$ and the X-ray flux F_x, for stars with $F_x \lesssim 10^6$ erg cm^{-2} s^{-1}

$$\dot{M}/A_\star \propto F_x^{1.34}. \qquad (1)$$

Because stars, as they age, rotate more slowly and because their activity decreases with rotation, X-ray fluxes also decay with age (e.g. Guedel 2004). Thus, the $\dot{M} - F_x$ relation implies that stars that are younger and have larger F_x, should also have higher $\dot{M}$. This, consequently, can have important effects on the early evolution of planetary systems. For example, extrapolations using equation (1) suggest that the 700 Myr-Sun would have had $\dot{M}$ that is ~100 times larger than the current solar mass-loss rate $\dot{M}_\odot = 2 \times 10^{14}$ M$_\odot$ yr^{-1} (Wood et al. 2005b). If this is indeed the case, this can explain the loss of the Martian atmosphere as due to erosion caused by the stronger wind of the young Sun (Wood 2004).

However, more active stars with $F_x \gtrsim 10^6$ erg cm^{-2} s^{-1} do not obey equation (1) – their derived $\dot{M}$ are several orders of magnitude smaller than what equation (1) predicts (Wood et al. 2005b, 2014). What could cause the change in wind characteristics at $F_x \sim 10^6$ erg cm^{-2} s^{-1}? Wood et al. (2005b) hypothesized that the stars to the right of the 'wind dividing line' (WDL; i.e. with $F_x \gtrsim 10^6$ erg cm^{-2} s^{-1}) have a concentration of spots at high latitudes, as recognized in Doppler Imaging studies (e.g. Strassmeier 2009), which could influence the magnetic field geometry of the star. They argue that these objects might possess a strong dipole component (or strong toroidal fields, Wood & Linsky 2010) 'that could envelope the entire star and inhibit stellar outflows'.

In this Letter, we investigate the hypothesis that solar-type stars to the right of the WDL should have a distinct magnetic field topology compared to the stars to the left of the WDL. For that, we select stars in Wood et al. sample that have large-scale surface magnetic fields previously reconstructed through Zeeman–Doppler Imaging (ZDI). In our analysis, only the large-scale surface fields are considered and we cannot assess if something happening at a smaller magnetic scale can affect the $\dot{M} - F_x$ relation.

2 MAGNETIC FIELD RECONSTRUCTION

Our sample consists of seven objects (Table 1) out of 12 dwarf stars (not considering the Sun) in Wood et al. sample.

The large-scale magnetic fields were observationally-derived through the ZDI technique (Morin et al. 2008; Morgenthaler et al. 2012; Jeffers et al. 2014; Petit et al., in preparation; Boro Saikia et al., in preparation; Boisse et al., in preparation). This technique consists of reconstructing the stellar surface magnetic field based on a series of circularly polarized spectra (Donati & Brown 1997). In its most recent implementation, ZDI solves for the radial B_r, meridional B_θ and azimuthal B_φ components of the stellar magnetic field, expressed in terms of spherical harmonics and their colatitude-derivatives (Donati et al. 2006b)

$$B_r(\theta, \varphi) = \sum_{lm} \alpha_{lm} P_{lm} e^{im\varphi}, \qquad (2)$$

$$B_\theta(\theta, \varphi) = \sum_{lm} \left[\frac{\beta_{lm}}{l+1} \frac{dP_{lm}}{d\theta} + \frac{\gamma_{lm}}{l+1} \frac{im}{\sin\theta} P_{lm} \right] e^{im\varphi}, \qquad (3)$$

Table 1. Properties of the stars considered in this work. Rotation periods P_{rot} were derived in the associated ZDI work (references in Table 2), while the remaining values are from Wood 2004, Wood & Linsky 2010, Wood et al. 2014. Note that F_x, $\dot{M}$ and the magnetic maps are not necessarily derived at the same observational epoch.

Star ID	Sp. type	$R_\star$ (R$_\odot$)	P_{rot} (d)	F_x (10^5 erg s^{-1} cm^{-2})	$\dot{M}$ (M$_\odot$)
EV Lac	M3.5V	0.35	4.4	130	1.0
ξ Boo A	G8V	0.83	5.6	17	0.5
π^1 UMa	G1.5V	0.95	5.0	17	0.5
ϵ Eri	K1V	0.78	10.3	5.6	30.0
ξ Boo B	K4V	0.61	10.3	4.1	4.5
61 Cyg A	K5V	0.68	34.2	1.0	0.5
ϵ Ind	K5V	0.75	37.2	0.72	0.5
Sun	G2V	1.00	25.0	0.32^a	1.0

Note. ^{a}Within its cycle, the Sun's X-ray luminosity varies from $\simeq 0.27$ to 4.7×10^{27} erg s^{-1} (Peres et al. 2000), corresponding to $F_x = 4.4 \times 10^4$ and 7.7×10^5 erg cm^{-2} s^{-1}, respectively. For consistency, we chose however to use the same value as used in Wood et al. (2014), which is more representative of the Sun at minimum.

$$B_\varphi(\theta, \varphi) = -\sum_{lm} \left[\frac{\beta_{lm}}{l+1} \frac{im}{\sin\theta} P_{lm} - \frac{\gamma_{lm}}{l+1} \frac{dP_{lm}}{d\theta} \right] e^{im\varphi}, \qquad (4)$$

where α_{lm}, β_{lm}, γ_{lm} are the coefficients that provide the best fit to the spectropolarimetric data and $P_{lm} \equiv P_{lm}(\cos\theta)$ is the associated Legendre polynomial of degree l and order m.

To quantify the magnetic characteristics of the stars in our sample, we compute the following quantities (Table 2):

(i) the average squared magnetic field (i.e. proportional to the magnetic energy): $\langle B^2 \rangle = \frac{1}{4\pi} \int (B_r^2 + B_\theta^2 + B_\varphi^2) \sin\theta \, d\theta d\varphi$.

(ii) The average squared poloidal component of the magnetic field $\langle B_{pol}^2 \rangle$ and its fraction $f_{pol} = \langle B_{pol}^2 \rangle / \langle B^2 \rangle$. To calculate $\langle B_{pol}^2 \rangle$, we neglect terms with γ_{lm} in equations (3) and (4).

(iii) The axisymmetric part of the poloidal energy $\langle B_{axi}^2 \rangle$ and its fraction with respect to the poloidal component $f_{axi} = \langle B_{axi}^2 \rangle / \langle B_{pol}^2 \rangle$. To calculate $\langle B_{axi}^2 \rangle$, we restrict the sum of the poloidal magnetic field energy to orders $m = 0$, $m < l/2$.

(iv) The average squared toroidal component of the magnetic field $\langle B_{tor}^2 \rangle = \langle B^2 \rangle - \langle B_{pol}^2 \rangle$ and its fraction $f_{tor} = 1 - f_{pol}$.

(v) The average squared dipolar component of the magnetic field $\langle B_{dip}^2 \rangle$ and its fraction $f_{dip} = \langle B_{dip}^2 \rangle / \langle B^2 \rangle$. To calculate $\langle B_{dip}^2 \rangle$, we restrict the sum of the total magnetic field energy (i.e. including the three components of $\boldsymbol{B}$) to degree $l = 1$.

Similarly to the Sun, it has been recognized that stellar magnetism can evolve on an yearly time-scale, with some stars exhibiting complete magnetic cycles. Three of the objects in our sample, namely EV Lac, ξ Boo A and ϵ Eri, have multi-epoch reconstructed surface maps. For these stars, f_{pol}, f_{axi}, f_{dip} and $\langle B^2 \rangle$, which are shown in Table 2, were averaged over multiple observing epochs (see Appendix A). We note that, as the observations are not done at regular time intervals, the time the star spends in a given 'magnetic state' might not be well represented by this simple average. However, we believe that this approach is a better representation of the magnetic characteristic for each of these stars over the choice of one single-epoch map, in particular when the star-to-star differences are comparable to the year-to-year (i.e. amplitude) variations that stars exhibit (more important in the most active stars).

Table 2. Magnetic properties of our sample. EV Lac, ξ Boo A and ε Eri had their properties averaged over multi-epochs (Appendix A).

| Star ID	$\langle B^2 \rangle$ (G^2)	$\langle B_{\rm pol}^2 \rangle$ (G^2)	$\langle B_{\rm tor}^2 \rangle$ (G^2)	$\langle B_{\rm axi}^2 \rangle$ (G^2)	$\langle B_{\rm dip}^2 \rangle$ (G^2)	$f_{\rm pol}$	$f_{\rm tor}$	$f_{\rm axi}$	$f_{\rm dip}$	Reference for surface magnetic map
EV Lac	3.6×10^5	3.4×10^5	1.7×10^4	1.0×10^5	2.5×10^5	0.95	0.05	0.31	0.72	Morin et al. (2008)
ξ Boo A	1.8×10^3	6.6×10^2	1.1×10^3	3.4×10^2	1.2×10^3	0.37	0.63	0.51	0.43	Morgenthaler et al. (2012)
π^1 UMa	1.1×10^3	2.0×10^2	8.9×10^2	3.3×10^1	7.4×10^2	0.18	0.82	0.16	0.68	Petit et al. (in preparation)
ε Eri	2.7×10^2	2.0×10^2	7.5×10^1	7.8×10^1	2.0×10^2	0.72	0.28	0.40	0.75	Jeffers et al. (2014)
ξ Boo B	4.0×10^2	2.7×10^2	1.3×10^2	7.3×10^1	1.8×10^2	0.68	0.32	0.27	0.45	Petit et al. (in preparation)
61 Cyg A	4.5×10^1	3.9×10^1	5.7×10^0	8.2×10^{-1}	8.6×10^0	0.87	0.13	0.02	0.19	Boro Saikia et al. (in preparation)
ε Ind	5.8×10^2	5.6×10^2	2.0×10^1	2.8×10^2	3.3×10^2	0.96	0.04	0.51	0.56	Boisse et al. (in preparation)
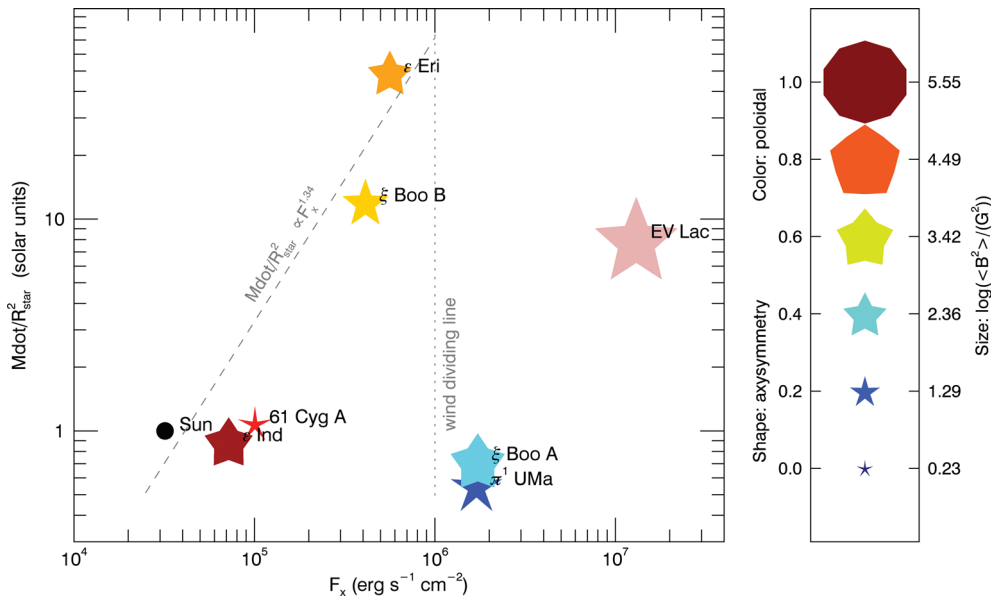
Figure 1. Mass-loss rates per surface area versus X-ray fluxes showing only the stars for which we have reconstructed surface fields. Symbol sizes are proportional to log $\langle B^2 \rangle$, their colours indicate the fractional poloidal energy (ranging from deep red for purely poloidal field $f_{\rm pol} = 1$ to blue for purely toroidal field $f_{\rm pol} = 0$), and their shapes indicate the fraction of axisymmetry of the poloidal component (ranging from a decagon for purely axisymmetric field $f_{\rm axi} = 1$ to a point-shaped star for $f_{\rm axi} = 0$). The $\dot{M} - F_{\rm x}$ relation (equation 1) is shown as a dashed line and the WDL at $F_{\rm x} = 10^6$ erg cm^{-2} s^{-1} is shown as a dotted line. The Sun (filled black circle) is shown for comparison.

3 MAGNETIC FIELDS AS THE CAUSE OF THE BREAK IN THE $\dot{M} - F_{\rm X}$ RELATION

One proposed idea for the break in the $\dot{M} - F_{\rm x}$ relation for the most active stars is that stars that are to the right of the WDL have surface magnetic field topologies that are significantly different, with either stronger dipolar (Wood et al. 2005b) or toroidal fields (Wood & Linsky 2010), that partially inhibit the outflow of the stellar wind, giving rise to reduced $\dot{M}$. To verify the first hypothesis, we compute $\langle B_{\rm dip}^2 \rangle$ and $f_{\rm dip}$ for all the stars in our sample (Table 2). We do not find any particular evidence that stars to the right of the WDL, namely π^1 UMa, ξ Boo A and EV Lac, have dipolar magnetic fields whose characteristics are remarkably different from the remaining stars in our sample.

Fig. 1 presents a similar version of Wood et al. diagram ($\dot{M}/A_{\star}$ versus $F_{\rm x}$) showing only the stars for which we have reconstructed surface fields. The symbols are as in fig. 3 of Donati & Landstreet (2009), in which their sizes are proportional to log $\langle B^2 \rangle$, their colours are related to $f_{\rm pol}$, and their shapes to $f_{\rm axi}$ (see caption of figure). EV Lac is included in this plot for completeness but it is not considered in the analysis that follows. It has been argued that EV Lac could be a discrepant data point in the wind-activity relation because it is the least solar-like star in the sample (Wood 2004). Indeed, it

has been revealed that the magnetism of active M dwarf stars, like EV Lac, has striking differences from solar-like objects, both in intensity and geometry (Donati et al. 2006a, 2008; Reiners & Basri 2007; Reiners, Basri & Browning 2009; Morin et al. 2008, 2010). Note that, except for EV Lac, our objects have Rossby numbers Ro > 0.1, where Ro is defined as the ratio between the convective turnover time-scale to the rotation period of the star (Ro compiled by Vidotto et al. 2014b). Therefore, none of our solar-type stars are in the X-ray saturated regime (Pizzolato et al. 2003).

Fig. 1 shows no evidence that $\dot{M}$ and $f_{\rm axi}$ (symbol shape) are related, indicating that the axisymmetry of the poloidal field cannot explain the wind-activity relation nor its break. In the Sun, $\dot{M}$ and $f_{\rm axi}$ also seem to be unrelated. The solar dipolar field, nearly aligned with the Sun's rotation axis (and therefore nearly axisymmetric) at minimum activity phase, increasingly tilts towards the equator as the cycle approaches activity maximum (DeRosa, Brun & Hoeksema 2012), decreasing therefore $f_{\rm axi}$. In spite of the cycle variation of $f_{\rm axi}$ in the Sun, the solar wind mass-loss rates remains largely unchanged (Wang 2010).

What stands out in Fig. 1 is that solar-type stars with larger toroidal fractional fields (bluer) are concentrated to the right of the WDL. With the limited number of stars with both ZDI and wind
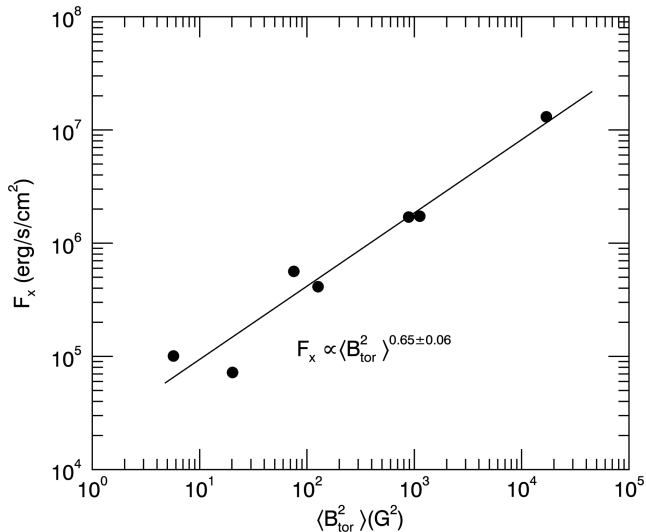
Figure 2. Relation between F_x and $\langle B_{tor}^2 \rangle$ does not show a break at $F_x \sim 10^6$ erg cm^{-2} s^{-1}. Solid line is a power law fit the data. Because $\langle B_{tor}^2 \rangle$ and $\langle B_{pol}^2 \rangle$ are correlated (See et al. 2015), correlations between F_x and $\langle B_{pol}^2 \rangle$ or $\langle B^2 \rangle$ also exist (see Table 3).

Table 3. Slope of the ordinary least-squares fits to the logarithm of our data (i.e. $y \propto x^{slope}$).

y(x)	$F_x(\langle B_{tor}^2 \rangle)$	$F_x(\langle B_{pol}^2 \rangle)$	$F_x(\langle B_{dip}^2 \rangle)$	$F_x(\langle B^2 \rangle)$
slope	0.65 ± 0.06	0.47 ± 0.05	0.50 ± 0.03	0.55 ± 0.04

measurements, there is no evidence at present for a sharp transition in magnetic topology across the WDL. Instead, the concentration of stars with dominantly toroidal fields to the right of the WDL reflects a trend towards more strongly toroidal fields with increasing F_x, which is in turn associated with rapid rotation. Petit et al. (2008) showed that, as stellar rotation increases, solar-type stars tend to have higher fraction of toroidal fields (symbols becoming increasingly bluer in diagrams such as the one expressed in Fig. 1; see also fig. 3 in Donati & Landstreet 2009). Since rotation is linked to activity, it is not surprising that π^1 UMa and ξ Boo A, the most active and rapidly rotating solar-type stars in our sample, are the ones with the largest fraction of toroidal fields. To confirm our findings, it is essential to perform further wind measurements and ZDI observations of more stars at both sides of the break.

We note also that if instead of plotting F_x in the x-axis of Fig. 1, we plotted $\langle B_{tor}^2 \rangle$, this plot would present the same general property: $\dot{M}/A_\star$ that increases with $\langle B_{tor}^2 \rangle$ for the least active stars and then a break in this relation for π^1 UMa and ξ Boo A, with the break occurring somewhere between $\langle B_{tor}^2 \rangle \sim 200$ and 800 G^2.[1] The similar characteristics between $\dot{M}/A_\star$ versus F_x and $\dot{M}/A_\star$ versus $\langle B_{tor}^2 \rangle$ is because $\langle B_{tor}^2 \rangle$ is correlated to F_x, as shown in Fig. 2 (this figure includes EV Lac). Because $\langle B_{tor}^2 \rangle$ and $\langle B_{pol}^2 \rangle$ are correlated (See et al. 2015), correlations between F_x and $\langle B_{pol}^2 \rangle$ or $\langle B^2 \rangle$ also exist (see Table 3). No break is seen in any of the F_x – magnetic energy relations. Because magnetism and X-ray flux evolve on $\sim$yearly time-scales, intrinsic variability is expected to increase the spread in all the relations in Table 3, further reinforcing the importance of multi-epoch ZDI observations.

---

[1] The same characteristic is seen in a plot of $\dot{M}/A_\star$ versus $1/$Ro, since F_x and Ro are anticorrelated (e.g. Stepien 1994).

Another important point to consider is that very active stars can jump between states with highly toroidal fields and mostly poloidal fields (Petit et al. 2009; Morgenthaler et al. 2012; Boro Saikia et al. 2015). Therefore, if the high fraction of toroidal magnetic fields is related to the break on the $\dot{M} - F_x$ relation, there may be some significant scatter in magnetic field topology on the right of the WDL, e.g. during $\sim$5 yr of observations, the fractional toroidal field of ξ Boo A varied between $f_{tor} \simeq 33$ per cent to 81 per cent, with an average of 63 per cent, giving this star a blueish colour in Fig. 1 (Appendix A). If this star were observed only during an epoch where its field is dominantly poloidal, the trend that stars to the right of the WDL are more toroidal (bluer) would not be recovered. This further strengthens the need of multi-epoch ZDI observations (cf. Section 2).

Assuming that a change in magnetic field topology is such that it will significantly affect the mass-loss rates of stellar winds, it would still take on the order of a few years (depending on the size of the astrosphere) for stellar winds to propagate out into the astrosphere boundary, where the Lyman α photons are absorbed. Therefore, simultaneous derivations of mass-loss rate (through Lyman α absorption) and magnetic field topology (through ZDI) are likely not going to be linked to each other. It would, nevertheless, be interesting to monitor both Lyman α absorption and magnetic topologies to see whether variations of the latter mimic those of the former with a $\sim$ few years delay.

4 CONCLUSIONS AND DISCUSSION

In this Letter, we have investigated if stellar magnetic fields could be the cause of the break in the wind-activity ($\dot{M} - F_x$) relation, for stars with $F_x \gtrsim 10^6$ erg cm^{-2} s^{-1} (Wood et al. 2005b). Our sample consisted of stars observed by Wood et al. that also had observationally-derived large-scale magnetic fields (Morin et al. 2008; Morgenthaler et al. 2012; Jeffers et al. 2014, Petit et al., in preparation; Boro Saikia et al., in preparation; Boisse et al., in preparation).

Wood et al. (2005b) and Wood & Linsky (2010) suggested that the break in the $\dot{M} - F_x$ relation seen for the most active stars could be caused by the presence of strong dipolar or toroidal fields that would inhibit the wind generation. In our analysis, we did not find any particular evidence that the dipolar field characteristics (or the degree of axisymmetry of the poloidal field) change at the WDL. We found that solar-type stars to the right of the WDL (namely ξ Boo A and π^1 UMa) have higher fractional toroidal fields (blueish points in Fig. 1), but no break or sharp transition is found (Fig. 2, Petit et al. 2008).

We also showed that there is a correlation between F_x and magnetic energy (Table 3), which implies that $\dot{M}$ – magnetic energy relation has the same general properties as the original $\dot{M} - F_x$ relation (i.e. a positive correlation for $F_x \lesssim 10^6$ erg cm^{-2} s^{-1}, followed by a break). Contrary to the $\dot{M} - F_x$ relation, no break at the WDL is seen in the F_x – magnetic energy relations.

We note that very active stars can jump between states with highly toroidal fields and mostly poloidal fields (Petit et al. 2009; Morgenthaler et al. 2012; Boro Saikia et al. 2015). If magnetic fields are actually affecting stellar winds (i.e. the high fraction of toroidal fields is related to the break in the $\dot{M} - F_x$ relation), there may be some significant scatter in magnetic field topology on the right of the WDL, even for a given star observed at various phases of its magnetic cycle.

We finally add that the break in the $\dot{M} - F_x$ relation found by Wood et al. (2005b) is at odds with some theoretical works on

stellar winds and empirically-derived relations used to compute outflow rates ($\dot{M}_{\mathrm{CME}}$) of coronal mass ejections (CMEs). The time-dependent stellar wind models of Holzwarth & Jardine (2007); See et al. (2014); Johnstone et al. (2015) predict a different (in general, weaker) dependence of $\dot{M}$ with F_{x} than that of equation (1) and do not predict a sharp decrease in $\dot{M}$ for stars to the right of the WDL. These models use empirical data on rotation, wind temperature, density and magnetic field strength to constrain theoretical wind scenarios. They are, however, limited to one or two dimensions and cannot, therefore, incorporate the 3D nature of stellar magnetic fields. 3D stellar wind studies that incorporates observed stellar magnetic maps have been carried out but they are currently not time-dependent (Cohen et al. 2010; Vidotto et al. 2012, 2014a; Jardine et al. 2013).

Other theoretical works suggested that CMEs could be the dominant form of mass-loss for active stars (Aarnio, Matt & Stassun 2012; Drake et al. 2013; Osten & Wolk 2015). These works predicted that $\dot{M}_{\mathrm{CME}} \gtrsim 100 \mathrm{M}_{\odot}$ for active solar-like stars, in contradiction to the results found by Wood et al. for active stars such as π^1 UMa and ξ Boo A. A possibility for this disagreement is that the solar CME-flare relation cannot be extrapolated all the way to active stars (Drake et al. 2013). Drake et al. (2013) suggested that there might not be a one-to-one relation between observed stellar X-ray flares and CMEs. They argue that on active stars, CMEs are more strongly confined, and so fewer of them are produced for any given number of X-ray flares. This stronger confinement could be caused by the noticeable differences between the solar and stellar magnetic field characteristics. What we have shown here is that indeed the most active stars seem to have more toroidal large-scale magnetic field topologies. Numerical modelling efforts would hopefully be able to shed light on whether the large-scale toroidal fields could indeed result in more confined CMEs.

ACKNOWLEDGEMENTS

REFERENCES

Aarnio A. N., Matt S. P., Stassun K. G., 2012, ApJ, 760, 9
Boro Saikia S., Jeffers S. V., Petit P., Marsden S., Morin J., Folsom C. P., 2015, A&A, 573, A17
Bouvier J., Matt S. P., Mohanty S., Scholz A., Stassun K. G., Zanni C., 2014, in Beuther H., Dullemond C. P., Klessen R. S., Henning T. K., eds, Protostars and Planets VI. Univ. Arizona Press, Tuscan, AZ, p. 433
Cohen O., Drake J. J., Kashyap V. L., Korhonen H., Elstner D., Gombosi T. I., 2010, ApJ, 719, 299
Debes J. H., 2006, ApJ, 652, 636
DeRosa M. L., Brun A. S., Hoeksema J. T., 2012, ApJ, 757, 96
Donati J., Landstreet J. D., 2009, ARA&A, 47, 333
Donati J., Forveille T., Cameron A. C., Barnes J. R., Delfosse X., Jardine M. M., Valenti J. A., 2006a, Science, 311, 633
Donati J. et al., 2006b, MNRAS, 370, 629
Donati J. et al., 2008, MNRAS, 390, 545
Donati J.-F., Brown S. F., 1997, A&A, 326, 1135
Drake J. J., Cohen O., Yashiro S., Gopalswamy N., 2013, ApJ, 764, 170
Gaidos E. J., Güdel M., Blake G. A., 2000, Geophys. Res. Lett., 27, 501

Gómez de Castro A. I., Verdugo E., 2007, ApJ, 654, L91
Guedel M., 2004, A&A Rev., 12, 71
Holzwarth V., Jardine M., 2007, A&A, 463, 11
Jardine M., Vidotto A. A., van Ballegooijen A., Donati J.-F., Morin J., Fares R., Gombosi T. I., 2013, MNRAS, 431, 528
Jeffers S. V., Petit P., Marsden S. C., Morin J., Donati J.-F., Folsom C. P., 2014, A&A, 569, A79
Johnstone C. P., Güdel M., Brott I., Lüftinger T., 2015, A&A, 577, A28
Kwan J., Edwards S., Fischer W., 2007, ApJ, 657, 897
Lim J., White S. M., 1996, ApJ, 462, L91
Morgenthaler A. et al., 2012, A&A, 540, A138
Morin J. et al., 2008, MNRAS, 390, 567
Morin J., Donati J., Petit P., Delfosse X., Forveille T., Jardine M. M., 2010, MNRAS, 407, 2269
Osten R. A., Wolk S. J., 2015, ApJ, 79, 12
Parsons S. G. et al., 2012, MNRAS, 420, 3281
Peres G., Orlando S., Reale F., Rosner R., Hudson H., 2000, ApJ, 528, 537
Petit P. et al., 2008, MNRAS, 388, 80
Petit P., Dintrans B., Morgenthaler A., van Grootel V., Morin J., Lanoux J., Aurière M., Konstantinova-Antova R., 2009, A&A, 508, L9
Pizzolato N., Maggio A., Micela G., Sciortino S., Ventura P., 2003, A&A, 397, 147
Reiners A., Basri G., 2007, ApJ, 656, 1121
Reiners A., Basri G., Browning M., 2009, ApJ, 692, 538
See V., Jardine M., Vidotto A. A., Petit P., Marsden S. C., Jeffers S. V., do Nascimento J. D., 2014, A&A, 570, A99
See V. et al., 2015, MNRAS, 453, 4301
Stepien K., 1994, A&A, 292, 191
Strassmeier K. G., 2009, A&A Rev., 17, 251
van den Oord G. H. J., Doyle J. G., 1997, A&A, 319, 578
Vidotto A. A., Fares R., Jardine M., Donati J.-F., Opher M., Moutou C., Catala C., Gombosi T. I., 2012, MNRAS, 423, 3285
Vidotto A. A., Jardine M., Morin J., Donati J. F., Opher M., Gombosi T. I., 2014a, MNRAS, 438, 1162
Vidotto A. A. et al., 2014b, MNRAS, 441, 2361
Villadsen J., Hallinan G., Bourke S., Güdel M., Rupen M., 2014, ApJ, 788, 112
Wang Y.-M., 2010, ApJ, 715, L121
Wargelin B. J., Drake J. J., 2002, ApJ, 578, 503
Wood B. E., 2004, Living Rev. Sol. Phys., 1, 2
Wood B. E., Linsky J. L., 2010, ApJ, 717, 1279
Wood B. E., Linsky J. L., Müller H., Zank G. P., 2001, ApJ, 547, L49
Wood B. E., Müller H.-R., Zank G. P., Linsky J. L., 2002, ApJ, 574, 412
Wood B. E., Redfield S., Linsky J. L., Müller H.-R., Zank G. P., 2005a, ApJS, 159, 118
Wood B. E., Müller H.-R., Zank G. P., Linsky J. L., Redfield S., 2005b, ApJ, 628, L143
Wood B. E., Müller H.-R., Redfield S., Edelman E., 2014, ApJ, 781, L33

SUPPORTING INFORMATION

Additional Supporting Information may be found in the online version of this article:

appendix.pdf
(http://www.mnrasl.oxfordjournals.org/lookup/suppl/doi:10.1093/mnrasl/slv147/-/DC1).

Please note: Oxford University Press is not responsible for the content or functionality of any supporting materials supplied by the authors. Any queries (other than missing material) should be directed to the corresponding author for the article.

This paper has been typeset from a TeX/LaTeX file prepared by the author.